



Implementation of Antenna Arrays One- and Two-Dimensional for Microwave Wireless Power Transfer Systems (MWPT)

Charanjeet Singh¹, Ramprakash Gupta²

Assistant Professor, Dept. of ECE, DCRUST, Murthal, Sonapat, Haryana, India¹

M. Tech Scholar, Dept. of ECE, DCRUST, Murthal, Sonapat, Haryana, India²

ABSTRACT: In this work, we exhibit novel one-and two-dimensional Antenna wire clusters for microwave remote power exchange (MWPT) frameworks. The radio wire cluster can be utilized as the MWPT getting reception apparatus of a coordinated MWPT and Bluetooth (BLE) correspondence module (MWPT-BLE module) for keen CNC (PC numerical control) shaft consolidated with the distributed computing framework SkyMars. The two-dimensional Antenna wire cluster has n lines of $1 \times m$ one-dimensional exhibit, in which every one-dimensional cluster is made out of various (m) differential sustaining radio wire units. Every differential bolstering radio wire unit has a microstrip receiving wire stripe. The stripe length is shorter than one wavelength to diminish the radio wire zone and to abstain from being eager to a high-arrange mode. A slant point of the principle pillar lines up with the broadside, and the primary shaft is additionally aggregated and contracted at the height bearing. At the operation recurrence of 9.9 GHz, the deliberate maximal E-plane pick up is 9.9 dB. Moreover, the deliberate maximal H-plane pick up and bar width are 9.66 dB and 27.5o, individually. The brilliant execution of the reception apparatus clusters shows that they are appropriate for MWPT frameworks.

KEYWORDS: CMOS, Antenna apparatus cluster, pick up, bar width, microwave remote power exchange (MWPT)

I.INTRODUCTION

Brilliant CNC (PC numerical control) axle is a vital point in Industry 4.0. At the point when the shaft, screw or instrument arrangement of the CNC is in operation, constant screen and small-scale tuning can be accomplished by reconciliation of the sensing and inciting smaller scale tuning advances of the sensors and miniaturized scale actuators. As of late, because of the quick improvement of versatile correspondence, web of things (IoT) and distributed computing advancements, sensor module with incorporated remote power exchange (WPT) and remote correspondence circuits for savvy CNC shaft has turned into a well-known research point. What's more, microwave WPT (MWPT), which shows high power change effectiveness (PCE) for a meter-level

separation, is appropriate for fueling the sensor module. Lamentably, no high pick up reception apparatus for MWPT framework has been accounted for. Accordingly, in this work, we exhibit novel one-and two-dimensional reception apparatus clusters [1], which can be utilized as MWPT getting radio wire of a coordinated MWPT and Bluetooth (BLE) correspondence sensor module (MWPT-BLE sensor module) for keen CNC shaft fused with the distributed computing framework Sky Mars [2]-[4].

International Journal of Advanced Research in Electrical, Electronics and Instrumentation Engineering

(An ISO 3297: 2007 Certified Organization)

Website: www.ijareeie.com

Vol. 6, Issue 6, June 2017

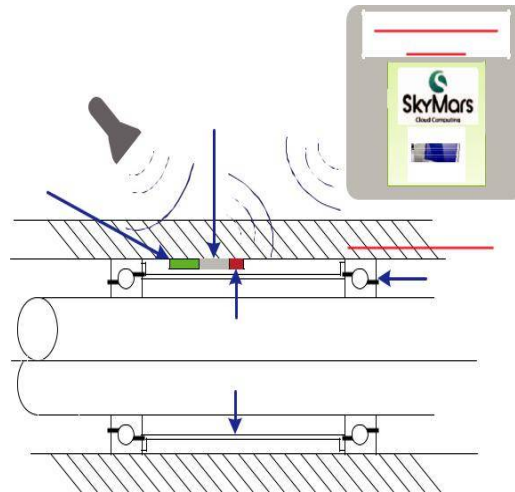


Fig. 1 Illustrative diagram of a smart spindle monitoring system.

II.MWPT-BLE SENSOR MODULE AND ANTENNA DESIGN

Fig. 1 is an illustrative graph of a keen shaft observing framework. The reception apparatus cluster in this work can be utilized as the MWPT getting receiving wire of the MWPT-BLE module for brilliant CNC shaft consolidated with the distributed computing framework SkyMars. The brilliant axle incorporates (non-contact cutting power, temperature, relocation, and vibration) sensors and miniaturized scale tuning instruments (coordinated on the apparatus framework and the turn shaft). The executed MWPT-BLE module is coordinated with the sensors to shape incorporated MWPT-BLE sensor modules, which are fueled by the inner MWPT framework. At the point when the axle, screw or instrument arrangement of the CNC is in operation, ongoing screen and smaller scale tuning can be accomplished by coordination of the sensing and inciting miniaturized scale tuning advancements of the sensors and small-scale actuators. Furthermore, rather than the customary metal shell, carbon fiber shell is utilized for the axle in this work. The outcome demonstrates the RF control constriction because of the carbon fiber shell is under 2 dBm (i.e. 37%), superior to that (8 dBm, i.e. 84.2%) of the conventional one which utilizes the metal shell.

Fig. 2 demonstrates the square graph of the proposed MWPT-BLE sensor module for keen CNC shaft consolidated with the distributed computing framework SkyMars. The contribution of the MWPT transmitting reception apparatus is irregular beat microwave control. This makes the concurrence of MWPT and remote

International Journal of Advanced Research in Electrical, Electronics and Instrumentation Engineering

(An ISO 3297: 2007 Certified Organization)

Website: www.ijareeie.com

Vol. 6, Issue 6, June 2017

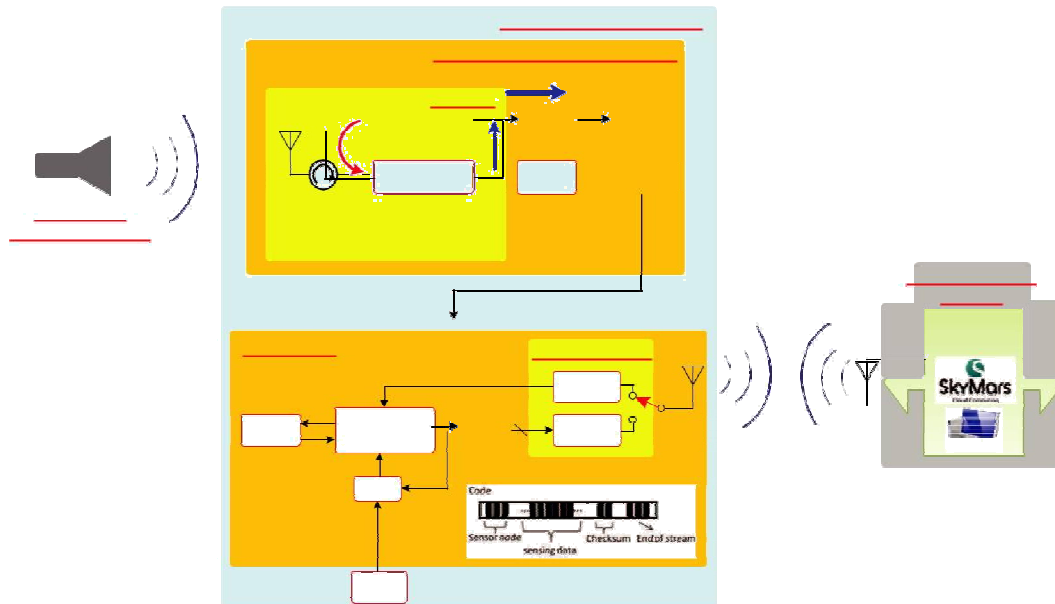


Fig. 2 Block diagram of the proposed MWPT-BLE sensor module, which is capable of MWPT and wireless communication.

of MWPT is the same as that of the BLE remote correspondence, i.e. 2.4 GHz, the impedance amongst MWPT and remote correspondence is insignificant. To diminish the receiving wire size of the MWPT framework, rather than operation recurrence of 2.4 GHz, 9.9 GHz is received in this work. Also, for the signs gotten by the MWPT accepting receiving wire, typically around 10-20% is reflected by its (load) amending circuit. Notwithstanding inadmissible PCE, the re-radiation of the reflected waves meddles with the remote correspondence. To defeat this inadequacy, in this work, we propose a MWPT framework with a circulator and a slave amending circuit in its rectenna (correcting radio wire) to reuse the reflected waves from the ace redressing circuit. In spite of the fact that the circulator itself brings about a 0.2-0.3 dB misfortune, the outcome demonstrates the impedance in remote correspondence can be successfully lessened, and a 10% improvement in general PCE can be accomplished.

The receiving wires in this work are planned and executed on RO4003 board. Fig. 3(a) demonstrates the arrangement perspective of the proposed non-high-arrange mode differential nourishing radio wire unit. It incorporates a differential nourishing structure and a

microstrip reception apparatus stripe. The differential nourishing structure has two ports. One port is the nourishing point, and the other port is associated with a differential circuit. The differential circuit has a transforming input (-) and a non-modifying input (+), separately, associated with the two sustaining terminals of the microstrip radio wire stripe. The flag stage distinction between the two encouraging terminals is 180 degree. The length L of the microstrip

International Journal of Advanced Research in Electrical, Electronics and Instrumentation Engineering

(An ISO 3297: 2007 Certified Organization)

Website: www.ijareeie.com

Vol. 6, Issue 6, June 2017

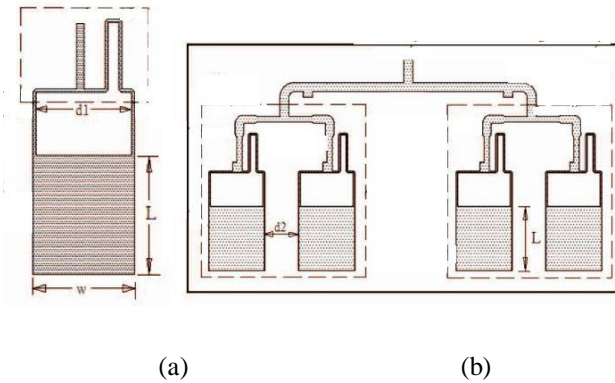


Fig. 3 (a) Plan view of the proposed non-high-order-mode differential feeding antenna unit. (b) Plan view of a one-dimensional antenna array, which includes 4 antenna units in (a).

antenna stripe is shorter than one wavelength λg (i.e. $L < \lambda g$).

In addition, the width (w) of the microstrip antenna stripe is equal to a half wavelength (i.e. $w = \lambda g / 2$). This leads to the gap d_1 between the two feeding terminals (-) and (+) of the microstrip antenna stripe is approximately

equal to a half wavelength (i.e. $d_1 \approx \lambda g / 2$).

Fig. 3(b) shows the plan view of the proposed 1x4 one-dimensional antenna array. The 1x4 one-dimensional antenna array has a RO4003 substrate, a power dividing circuit, a main feeding point, and a grounding layer. The main feeding point is connected to the power dividing circuit, which is connected to the four antenna units. The space d_2 between the two-adjacent differential feeding antenna units is a half wavelength (i.e. $d_2 = \lambda g / 2$). The

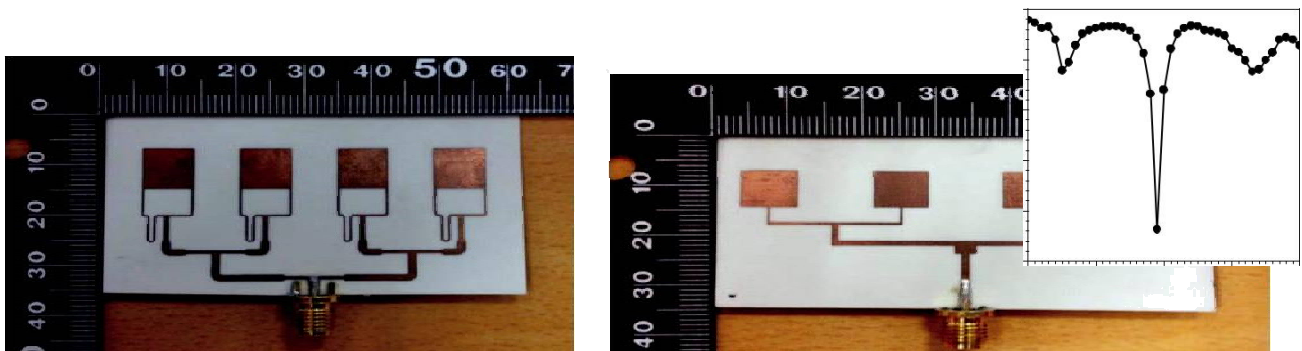


Fig. 4 Photographs of (a) the proposed differential feeding, and (b) the conventional single feeding 1 x 4 one-dimensional antenna array connected to a coaxial cable. (c) Measured S11 versus frequency characteristics of the proposed antenna array in (a).

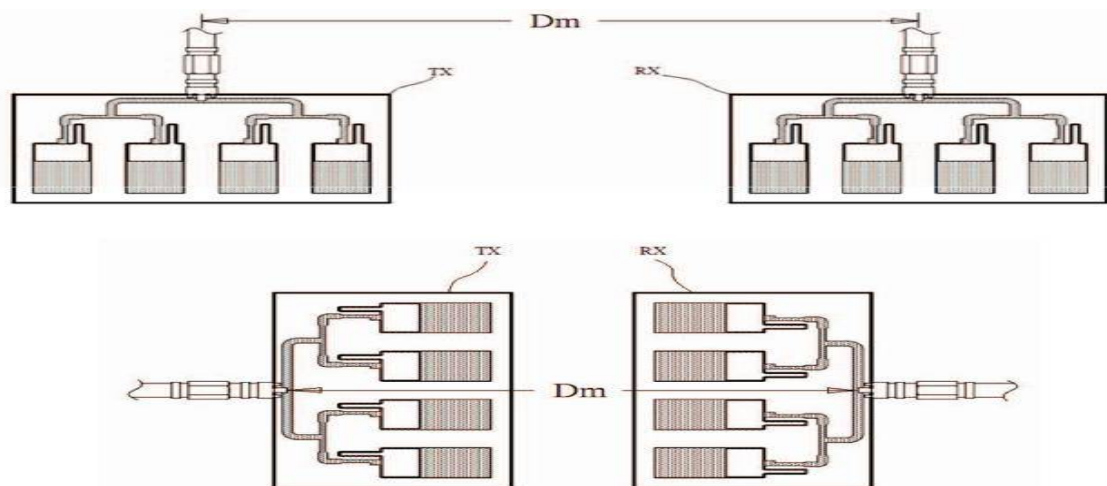
RO4003 substrate has two opposite planes. The four antenna units, the power dividing circuit, and the main feeding point are formed on the first plane. The grounding layer is formed on the other plane. The feeding circuits of the two one-to-two power dividers are connected to the power dividing circuit. Each of the two one-to-two power divider has a

feeding circuit, a first impedance match circuit with a $\lambda/4$ first length, and a second impedance match circuit with a $\lambda/4$ second length.

III. MEASUREMENT RESULTS AND DISCUSSIONS

The frequency-dependent S-parameter measurement was performed from 2 to 20 GHz by an Anritsu MS46322A vector network analyzer. Fig. 4(a) shows the photograph of the implemented differential feeding 1×4 one-dimensional antenna array. The area of the RO4003 board is about 6.2×3.5 cm². The main feeding point is connected to a coaxial cable for measurement of the input reflection coefficient (S11) and radiation patterns. To enhance the gain of each of the non-high-order-mode differential feeding antenna unit, the impedance of each of the two feeding terminals of the microstrip antenna stripe is 100

Ω . The impedance of the feeding point of the differential feeding structure is 50 Ω . The impedance of each of the inverting and non-inverting inputs (-) and (+) of each differential circuit is 100 Ω . The impedance of each feeding circuit of the power divider is 50 Ω , and the loading impedance of each of the first and second impedance match circuits is 70.7 Ω . This is the way to achieve an excellent S11 over the band of interest. For comparison, the corresponding conventional single feeding 1×4 one-dimensional antenna array is also designed and implemented for comparison, as shown in Fig. 4(b). The area of the RO4003 board is about 6.7×3.5 cm². Fig. 4(c) shows the measured S11 versus frequency characteristics of the one-dimensional antenna array in Fig. 4(a). At the operation frequency of 9.9 GHz, excellent measured S11 of -21.83 dB is achieved, better than that



(-15 dB) of the measured minimal S11 of the conventional antenna array in Fig. 4(b) (not shown here). This leads to an excellent antenna gain.

Fig. 5(a) shows the plan view of the first arrangement of dual-antenna system which includes two one-dimensional antenna arrays shown in Fig. 4(a). To reduce the even mode coupling between the microstrip antenna stripes of the antenna units, differential feeding structure is used in each antenna unit. In comparison with the conventional dual-antenna system using the one-dimensional radio wire clusters with single bolstering reception apparatus units in Fig. 4(b), the proposed one has the benefits of higher disengagement and more straightforward creation prepare (in light of the fact that an additional exact opening penetrating system is not required). For instance, at the separation (D_m) between the bolstering purposes of 9 cm, the deliberate disengagement is 56 dB, superior to that (46 dB) of the regular one.

Fig. 5(b) demonstrates the arrangement perspective of the second course of action of double reception apparatus framework which incorporates two **E-plane @9.9 GHz**

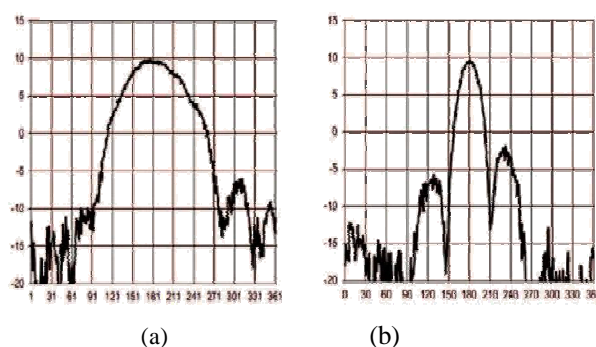


Fig. 6 Measured (a) E-plane, and (b) H-plane gain patterns of the one-dimensional antenna array in Fig. 4(a) at 9.9 GHz.

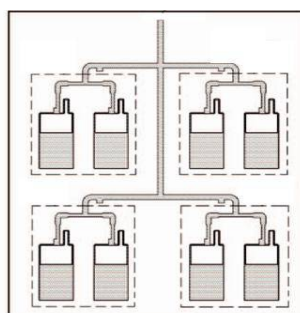


Fig. 7 Plane view of the proposed two- dimensional antenna array based on the one-dimensional antenna array in Fig. 4(a).

one-dimensional antenna arrays shown in Fig. 4(a). In comparison with the conventional dual-antenna system using the one-dimensional antenna arrays with single feeding antenna units in Fig. 4(b), the proposed one has the advantages of higher isolation and simpler fabrication process. For example, at Dm of 20 cm, the measured isolation is 47 dB, better than that (37 dB) of the conventional one.

The antennas in this work are placed in an anechoic chamber for radiation pattern measurement. An NSI-233 near-field scanner, which is capable of 1-18 GHz linear polarization measurement, is used. The E -plane radiation beam width is related to the number of the non-high-order-mode differential feeding antenna units. At the azimuth direction, the radiation beam of the dual-antenna system is concentrated. This leads to an enhancement in directivity. Figs. 6(a) shows the measured E-plane gain pattern of the one-dimensional antenna array in Fig. 4(a) at 9.9 GHz. The result shows the maximal E-plane gain is 9.9 dB. In addition, the E-plane beam width, i.e. the angle between the points at which the intensity is at half of its maximal value, is 78.6o. The H-plane radiation beam width is related to the length of the microstrip antenna stripe. At the elevation direction, the radiation beam of the dual-antenna system is concentrated and shrunk. This leads to an enhancement in directivity. Fig. 6(b) shows the measured H-plane gain patterns of the one-dimensional antenna array in Fig. 4(a) at 9.9 GHz. The result shows the maximal H-plane gain is 9.66 dB at 9.9 GHz. In addition, the H-plane beam width is 27.5o. In comparison with the conventional leaky-wave antenna array (with single feeding antenna unit), the proposed antenna array (with differential



International Journal of Advanced Research in Electrical, Electronics and Instrumentation Engineering

(An ISO 3297: 2007 Certified Organization)

Website: www.ijareeie.com

Vol. 6, Issue 6, June 2017

feeding antenna unit) can effectively reduce (or shrink) the beam width at the elevation direction, which leads to a better directivity. To the authors' knowledge, the achieved gain performance is one of the best gain results ever reported for a 10-GHz-band antenna.

Since the stripe length of the differential feeding antenna unit is shorter than one wavelength, in comparison with the leaky-wave antenna with stripe length of three times of the wavelength, the differential feeding antenna unit can further constitute a two-dimensional antenna array in a limited space. Fig. 7 shows the plan view of the designed 2×4 two-dimensional antenna array on a RO4003 board based on the one-dimensional antenna array shown in Fig. 4(a). The antenna units, the power dividing circuits and the main feeding point are formed on one plane of the RO4003 board, and the grounding layer is formed on the other plane of the RO4003 board. The 2×4 antenna units are arranged to 2 rows and 4 columns. The 2 power dividing circuits are respectively formed adjacent to the n row of the antenna units. The feeding circuit of the power divider of the antenna unit is connected to the power dividing circuit on the corresponding row.

IV. CONCLUSION

We demonstrate one- and two -dimensional antenna arrays suitable for MWPT receiving antenna applications. In comparison with the conventional antenna arrays with single feeding antenna units, better isolation and higher gain are achieved for the proposed one. In addition, in comparison with the conventional antenna array, which has microstrip antenna stripe length equals or longer than three times of the wavelength, smaller antenna size, better isolation and higher gain are achieved for the proposed one. These excellent results indicate the proposed antenna arrays are suitable for MWPT receiving antenna.

REFERENCES

- [1] TW invention patent No. 1385857.
- [2] WEISS Spindle Sensor Module with DRIVE-CLiQ and integrated Spindle Monitor, Brochure, Siemens AG2013(http://www.weissgmbh.com/uploads/media/Flyer_SMI24.pdf).
- [3] N. Suzuki, T. Mitani, and N. Shinohara, "Study and development of a microwave power receiving system for ZigBee device," Asia-Pacific Microwave Conference (APMC), pp. 45-48, 2010.
- [4] SkyMarsAPIXML3.03.pdf,SkymarsCloudComputingWebsite(<http://faremo.pmc.org.tw/RegisterServer/PageIndex.aspx?Language=TW>)